Extending dephasing time of nitrogen-vacancy center in diamond by suppressing nuclear spin noise

Xin-Yu Chen,[1,2] Chu-Dan Qiu,[3] Ya-Nan Lu,[4] Gang-Qin Liu,[4,5] Dong Ruan,[2] Feihao Zhang,[1,*] and Guilu Long[1,2,†]

[1]*Beijing Academy of Quantum Information Sciences, Beijing 100193, China*

[2]*Department of Physics, Tsinghua University, Beijing 100084, China*

[3]*Department of Physics, Southern University of Science and Technology, Shenzhen 518055, China*

[4]*Institute of Physics, Chinese Academy of Sciences, Beijing 100190, China*

[5]*Songshan Lake Materials Laboratory, Dongguan, Guangdong 523808, China*

(Received 2 March 2023; revised 22 July 2023; accepted 7 November 2023; published 29 November 2023)

Nitrogen-vacancy (NV) centers in diamond are a leading competitor for quantum sensing. The resolution of DC magnetic field sensing is limited by dephasing of the NV electron spin, with the main dephasing source being the thermal and quantum noise from the ^{13}C nuclear spin bath. In this work, we propose an effective method to extend the dephasing time of a single NV electron spin by suppressing the nuclear spin noise. On the one hand, we improve the technique of bath driving to accommodate nuclear spin bath decoupling, and extend the dephasing time from 2.6 to 10.2 μs at a magnetic field of 455 G. On the other hand, our method enables decoupling the quantum noise by inserting π rotations around the Z axis of the nuclear spin bath into the free evolution. By suppressing both the thermal and quantum noise, the dephasing time is extended by more than four times at 100 G. Our results provide a new route to explore strategies of suppressing the thermal noise and quantum noise in quantum information processing, and can be applied to other solid-state defects.

DOI: 10.1103/PhysRevB.108.174111

I. INTRODUCTION

The nitrogen-vacancy (NV) center in diamond is a potential platform for quantum sensing [1–3]. Physical quantities, such as magnetic field [4–6], electrical field [7,8], temperature [9–11], and pressure [12], can interact with the NV center and be measured at nanoscale. Among these applications, sensing of a DC magnetic field is of great significance in studying condensed matter [13–15] and biological processes [16–18].

The Ramsey experiment [19] of the NV electron spin is usually performed to measure the DC magnetic field, and the sensing precision is limited by dephasing. For NV ensembles, the main factor of dephasing is the interaction with paramagnetic substitutional nitrogen impurities (P1 centers). In high-purity samples, the dephasing is mainly caused by the interaction with the ^{13}C nuclear spin bath, the Overhauser field fluctuations of which have been observed in experiments [20,21]. According to the dephasing mechanism, the dephasing source can be divided into the thermal noise and the quantum noise [22], which can be modulated by adjusting the magnetic field [23,24]. At strong magnetic fields ($>$300 G) the thermal distribution of ^{13}C nuclear spins plays a main role in dephasing, while at medium magnetic fields ($1\,\mathrm{G} \lesssim B < 300\,\mathrm{G}$) the quantum fluctuation of nearby ^{13}C nuclear spins will also take effect.

Dynamic nuclear polarization (DNP) [25–30] is an effective method to suppress the thermal noise of ^{13}C nuclear spins. However, at weak or medium magnetic fields, the dynamical quantum noise can still dephase the electron spin. The isotope purification technique is useful for reducing the ^{13}C atoms [31,32], but a high degree of isotope purification is challenging. Bath driving [33–35] can also enhance the performance of DC magnetic sensing. It involves decoupling the P1 bath by inserting flip pulses of P1 centers in the middle of free evolution or driving the bath with a continuous wave. To further extend the dephasing time, the interaction with ^{13}C nuclear spins should be decoupled from the NV electron spin. However, as the gyromagnetic of the ^{13}C nuclear spins is orders of magnitudes smaller than P1 centers, the control time of the inversion pulse is much longer than the dephasing time of the electron spin, which hinders the application of bath driving.

The intrinsic ^{14}N nuclear spin of the NV center has been effectively utilized as a memory, leading to significant improvements in resolution for single-spin nuclear magnetic resonance spectroscopy [36,37]. In this work, we exploit the ^{14}N nuclear spin to store the coherence of the electron spin, thereby decoupling both the thermal and quantum noise from the entire ^{13}C nuclear spin bath in the Ramsey procedure. To address the thermal noise, we improve the technique of bath driving to facilitate the decoupling of the nuclear spin bath. By transferring the coherent state of the electron spin to the ^{14}N register, the long control time of the inversion gate inserted in the middle of free evolution will not cause dramatic dephasing. We experimentally demonstrate the proposal and extend the dephasing time from 2.6 to 10.2 μs at 455 G. In addition, by inserting π rotations around the Z axis of the nuclear spin bath into the free evolution, the quantum noise can be effectively suppressed. After decoupling both thermal and quantum noise experimentally, the dephasing time is extended

*zhangfh@baqis.ac.cn

†gllong@tsinghua.edu.cn

from 1.8 to 7.8 μs at 100 G. Our study can be combined with the isotope purification technique to improve DC magnetic field sensing, and will also be beneficial to other quantum information applications limited by dephasing.

II. DEPHASING IN THE NV SYSTEM

An NV center consists of a substitutional nitrogen atom and an adjacent vacancy in the diamond crystal lattice. Apart from the spin-1 electron spin and ^{14}N nuclear spin, there are spin-$1/2$ ^{13}C nuclear spins randomly distributed in the lattice with 1.1% natural abundance, which are potential qubits for quantum information processing, as well as the dephasing source for the electron spin. Applying a magnetic field B_z along [111]-crystallographic axis, the Hamiltonian of the NV electron spin interacting with the bath of ^{13}C nuclear spins can be described as

$$H_{\text{e-C}} = DS_z^2 + \gamma_e B_z S_z + \sum_j \gamma_C B_z I_z^j + \sum_{j,i} S_z A_i^j I_i^j, \tag{1}$$

where $D = 2\pi \times 2.87$ GHz is the electronic zero-field splitting, γ_e (γ_C) is the gyromagnetic ratio of the electron (nuclear) spin, subscript $i \in x, y, z$ denotes the axis of nuclear spin, A_i^j is the coupling strength between the electron spin and the jth ^{13}C nuclear spin, and S_z (I_i^j) is the spin-1 (spin-1/2) operator of the electron (jth nuclear) spin. The weak interactions between nuclear spins are neglected in the timescales considered here. The dephasing noise to the electron spin is caused by the coupling term in Eq. (1) and can be divided into thermal noise and quantum noise by dephasing mechanism [22]:

(i) *Thermal noise.* The diagonal part of the coupling term $\sum_j A_z^j I_z^j$ contributes a quasistatic noise $B_{\text{th}} = \sum_j A_i^j \langle I_z^j \rangle_b$ to the electron spin, where the angle bracket $\langle\cdot\rangle_b$ denotes an average over the bath state.

(ii) *Quantum noise.* The off-diagonal part of the coupling term $\sum_j (A_x^j I_x^j + A_y^j I_y^j)$ causes the dephasing of the electron spin by generating entanglement. At a strong magnetic field B_z, it can be suppressed by the Larmor precession $\sum_j \gamma_C B_z I_z^j$.

Applying a microwave with frequency ω_e, the detuning frequency $\Delta = D - \omega_e - \gamma_e B_z$ can be measured with the Ramsey experiment in the subspace of the electron spin, e.g., $m_S = 0$ and $m_S = -1$. In the Ramsey experiment, the electron spin is first prepared in a coherent state with a $\pi/2$ pulse. After a free evolution, a second $\pi/2$ pulse is applied before readout. From the readout signal, we can estimate the dephasing time T_2^* and the detuning frequency Δ, and therefore the magnetic field applied (Appendix A).

III. DECOUPLING THE THERMAL NOISE

Thermal noise is the main dephasing factor for the electron spin at strong magnetic fields [22]. Our method of decoupling the thermal noise is similar to bath driving. As sketched in Fig. 1(a), during the first free evolution ($\tau/2$), ^{13}C nuclear spins contribute a magnetic field B_{th} to the electron spin, and the electron spin will accumulate a phase θ_{th}. After the bath inversion pulse, the ^{13}C nuclear spins and thus the thermal noise are flipped, so the phases accumulated in the two free evolutions cancel each other out (Appendix A).

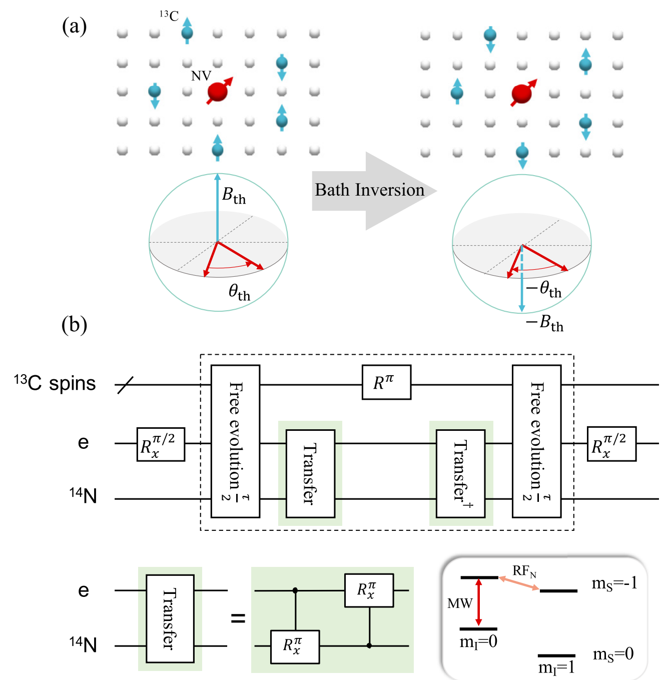

FIG. 1. The principle of decoupling the thermal noise. (a) The diagram of decoupling the thermal noise. The ^{13}C nuclear spins and thus the thermal noise (B_{th}) are flipped by the bath inversion pulse, and the phases (θ_{th}) accumulated in the two periods of free evolution cancel each other out. (b) The experimental sequence of decoupling the thermal noise. A π pulse (R^π) is applied to invert the ^{13}C bath in the middle of free evolution. The transfer operation is utilized to transfer the coherent state of the electron spin to the ^{14}N nuclear spin. Lower left panel: details of the transfer operation. Lower right panel: the energy levels of the electron spin ($m_S = 0, -1$) and the ^{14}N nuclear spin ($m_I = 1, 0$) used to form a two-qubit system. MW (RF_N) represents the conditional driving frequency of the electron (^{14}N nuclear) spin.

The decoupling sequence is shown in Fig. 1(b), where a radio-frequency (RF) π pulse (R^π) is applied to invert the ^{13}C bath midway through the Ramsey sequence. To overcome the problem that the duration of the inversion pulse is much longer than the dephasing time of the electron spin, we utilize the intrinsic ^{14}N nuclear spin as a register for coherence. We transfer the state of the electron spin to the ^{14}N nuclear spin before the inversion pulse and after we transfer back.

The energy levels of the electron spin and the ^{14}N nuclear spin used to form a two-qubit system are shown in the lower right panel of Fig. 1(b), where MW (RF_N) represents the conditional driving frequency of the electron (nuclear) spin. ^{14}N nuclear spin can be effectively polarized to $|1\rangle_\text{N}$ via the excited state level anticrossing (ESLAC) [38–40] at our applied magnetic field of 455 G. When outside the magnetic field range of ESLAC, the register spin can also be initialized with a "kick out" pulse [41] or swap-like gates [42]. The transfer operation is implemented as shown in the lower right panel of Fig. 1(b). The ^{14}N nuclear spin can be manipulated by decoherence-protected gates [43] or DDrf [44], in which the coherence of the electron spin is protected by dynamical

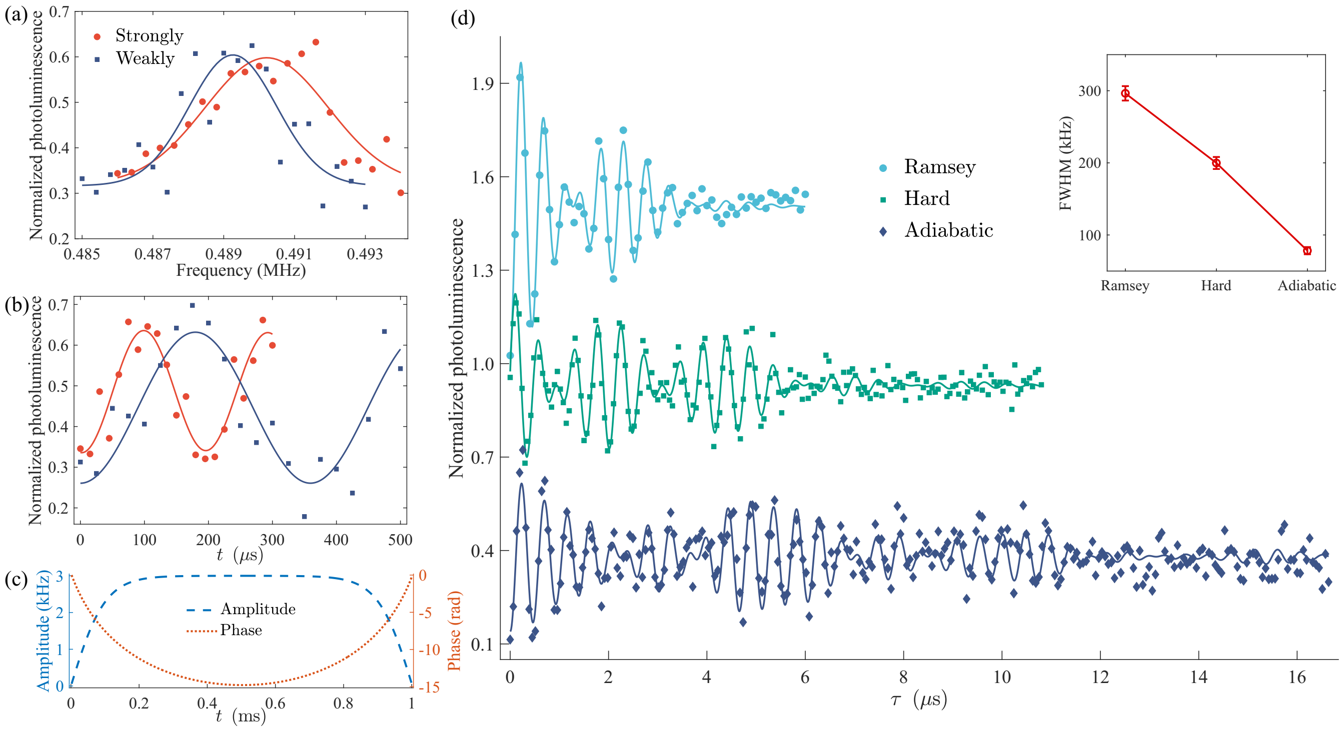

FIG. 2. Decoupling the quantum noise. (a), (b) Nuclear magnetic resonance and Rabi oscillation of two ^{13}C nuclear spins around the NV center. (c) The amplitude and phase of an adiabatic inversion pulse with the maximum amplitude set as 3 kHz and duration 1 ms. (d) Signals of the ordinary Ramsey method and after decoupling the thermal noise at a magnetic field of 455 G. Upper: Ramsey signal of the NV electron spin in our sample, and the dephasing time T_2^* is estimated to be 2.6(2) μs, where the number in the parentheses indicates the uncertainty in the last digit. Middle: We use a hard pulse to invert the bath, and T_2^* is extended to 5.4(8) μs. Lower: Utilizing adiabatic inversion pulse to invert the bath, T_2^* is extended further to 10.2(14) μs. We fit the experimental data by considering the strongly coupled ^{13}C nuclear spin. Inset: The FWHM of these three signals. The error bars are ±1 standard deviation.

decoupling (DD), while the nuclear spin is driven by $\mathrm{RF_N}$ during the time interval between the π pulses. The conditional gate on the electron spin C-R_x^π can be realized by a microwave with the strength of $A_\mathrm{N}/\sqrt{3}$ to cover the whole ^{13}C nuclear spin bath, where $A_\mathrm{N} = 2.16$ MHz is the coupling strength between the electron spin and the ^{14}N nuclear spin. More information about the transfer operation can be found in the Supplemental Material [45].

After the state is transferred, the electron spin will be in $|0\rangle_\mathrm{e}$, and all the weakly coupled ^{13}C nuclear spins will have the same resonance frequency. Therefore, we can flip the whole ^{13}C bath by an RF pulse, while the coherence stored in the ^{14}N nuclear spin is protected. It is worth noting that we actually have constructed a hybrid sensor: the electron spin is sensitive to the external magnetic field, while the ^{14}N nuclear spin has long coherence time.

To calibrate the control parameters of ^{13}C nuclear spins, we initialize and control strongly and weakly coupled ^{13}C nuclear spins with the method in [46]. Figures 2(a) and 2(b) are nuclear magnetic resonances and Rabi oscillations when the electron spin is in $|0\rangle_\mathrm{e}$, from which the resonance frequency and π pulse can be determined; see Supplemental Material for more details [45] (see also Refs. [47–49] therein). The large difference of Rabi frequency results from the g-tensor enhancement of the strongly coupled ^{13}C nuclear spin by the electron spin [50], while the resonance frequency deviates because of the magnetic field misalignment.

The comparison between the signals without and with our method are displayed in Fig. 2(d). The upper part shows the signal of the ordinary Ramsey method. The dephasing time T_2^* is estimated to be 2.6(2) μs, and the beat pattern results from the strongly coupled ^{13}C nuclear spin. The middle part of Fig. 2(d) shows that T_2^* is extended to 5.4(8) μs by the hard pulse. We can optimize the RF frequency, phase and duration of the hard pulse to get a better π pulse for the whole bath. Alternatively, we consider a shaped pulse of adiabatic inversion [51–53] as shown in Fig. 2(c), which is more robust against errors of control amplitude and of being off resonance [45]. With the shaped pulse, more nuclear spins can be inverted, and T_2^* is further extended to 10.2(14) μs in the lower part of Fig. 2(d). In this case, the beat signal is caused by the strongly coupled nuclear spin during the transfer operation. By fitting the Fourier transform spectra of these three signals [25,45], we extract the full width at half maximum (FWHM) linewidth in the inset of Fig. 2(d), which indicates a narrowing linewidth, leading to an improved resolution of DC magnetic field. The performance of our method is affected by gate fidelity, such as the fidelity of the transfer operation. The transfer efficiency will influence the signal amplitude and thus the signal-to-noise ratio. In addition, the off-diagonal part of the coupling term in Eq. (1) will cause extra noise because the

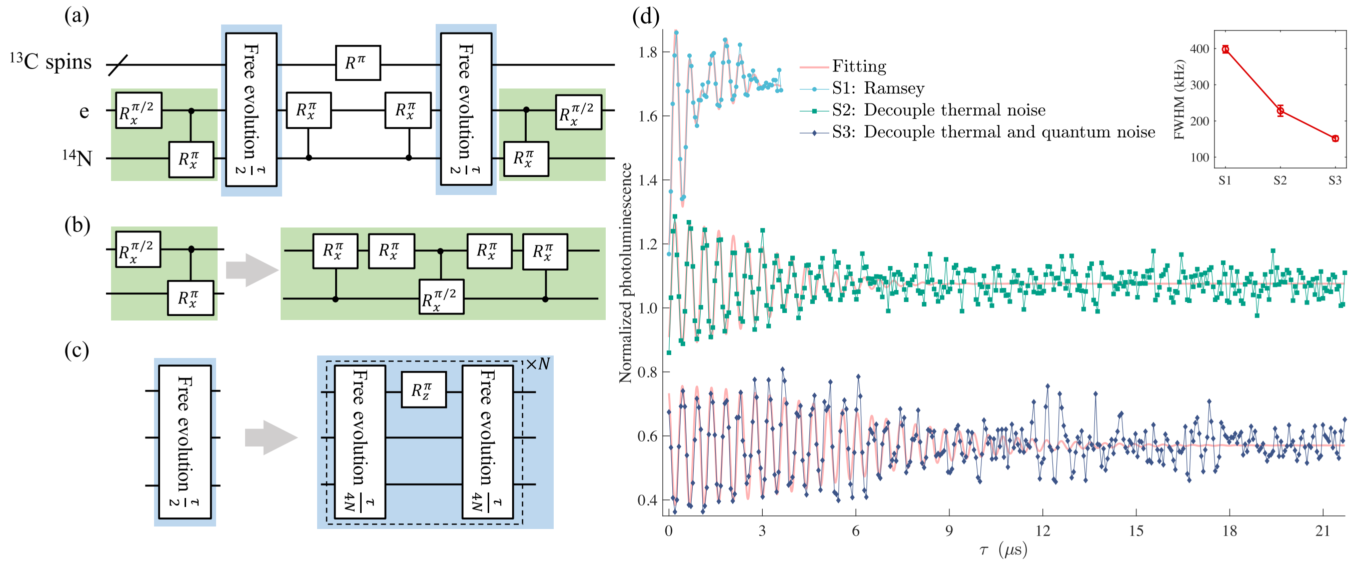

FIG. 3. Decoupling both the thermal and quantum noise. (a) The experimental sequence of decoupling both the thermal and quantum noise. The swap-like gates to polarize the ^{14}N nuclear spin are not shown. (b) The entanglement operation can be realized by hard pulses. (c) Inserting an R_z^π gate in the middle of every free evolution to suppress the quantum noise, where the circuit in the dashed box is repeated N times. (d) The experimental results at a magnetic field of 100 G. Upper: The signal of the ordinary Ramsey method (S1). T_2^* is estimated to be 1.8(1) μs. Middle: Signals after decoupling the thermal noise (S2). T_2^* is extended to 4.2(5) μs. Lower: Signals after decoupling both the thermal and quantum noise (S3). We insert eight R_z^π gates, and T_2^* is extended further to 7.8(9) μs. The fitting function is $S(\tau)=\sum_i^n A_i\cos(\omega_i\tau+\phi_i)\mathrm{e}^{-(\tau/T_2^*)^2}+C$, with $n=3$ for S1 and $n=1$ for S2 and S3. Inset: The FWHM of these three signals. The error bars are ±1 standard deviation.

Hamiltonians of the ^{13}C nuclear spin bath during the free evolution and during the transfer operation are noncommuting. At our applied magnetic field of 455 G, the noise caused by the weakly coupled ^{13}C nuclear spins can be suppressed by the Larmor precession. Other limitations include the temperature drifts, heating effect from the pulses, magnetic fluctuations, and so on.

IV. DECOUPLING THE QUANTUM NOISE

When the external magnetic field gets weaker, the off-diagonal part of the coupling term in Eq. (1) will be comparable to the Larmor precession and also dephase the electron spin, and the noise caused by the transfer operation in Fig. 1(b) will get noticeable. Therefore, we propose a method to suppress the off-diagonal part at a medium magnetic field.

To reduce the noise during the transfer operation, we upgrade the experimental sequence, as illustrated in Fig. 3(a). We move the conditional gate on the ^{14}N nuclear spin in the transfer operation to the green box to entangle the two spins, in which case we only need a conditional gate C-R_x to drive the electron spin to $|0\rangle_\mathrm{e}$ and the accumulated phase in the free evolution ($\tau/2$) will be stored in the ^{14}N nuclear spin. The operation in the green box can also be realized by hard pulses, as shown in Fig. 3(b). To further suppress the quantum noise during phase accumulation, we divide the free evolution into N pieces and insert an R_z^π pulse in the middle of each piece, as described in Fig. 3(c). In the subspace of $m_S=-1$, the evolution of the jth ^{13}C nuclear spin will become

$$U_1^j\left(\frac{\tau}{4N}\right)R_z^\pi U_1^j\left(\frac{\tau}{4N}\right)\approx\left[\mathbb{I}-\frac{i\left(\gamma_\mathrm{C}B_zI_z^j-A_z^jI_z^j\right)\tau}{2N}\right]R_z^\pi, \quad (2)$$

where $U_1^j(\tau/4N)=\exp[-i(\gamma_\mathrm{C}B_zI_z^j-A_x^jI_x^j-A_y^jI_y^j-A_z^jI_z^j)\tau/4N]$, which means the off-diagonal part is decoupled to the first order. The approximations hold true when $A_{x/y/z}^j\tau/4N\ll 1$, so we can get a better decoupling effect by dividing the whole evolution into more pieces (Appendix B).

The R_z^π gate can be realized by a free precession of $\pi/\gamma_\mathrm{C}B_z$, before which a conditional gate is utilized to drive the electron spin to $|0\rangle_\mathrm{e}$, so that all the ^{13}C nuclear spins will precess at a speed of $\gamma_\mathrm{C}B_z$. When the magnetic field is not too weak, we can also use a DD sequence to approximate the R_z^π gate, such as XY8 [54,55], which is robust against pulse errors. The DD sequence can decouple the electron spin and the spin bath, and the jth ^{13}C nuclear spin will get an average Hamiltonian

$$H_\mathrm{avg}=\left(\gamma_\mathrm{C}B_z-\frac{A_z^j}{2}\right)I_z^j-\frac{A_x^j}{2}I_x^j-\frac{A_y^j}{2}I_y^j. \quad (3)$$

If we select the total time of DD to be $\pi/\gamma_\mathrm{C}B_z$, the jth ^{13}C nuclear spin will realize a rotation along $(A_x^j/2, A_y^j/2, \gamma_\mathrm{C}B_z-A_z^j/2)$ with a degree of $\omega_\mathrm{avg}\pi/\gamma_\mathrm{C}B_z$, where $\omega_\mathrm{avg}=\sqrt{(\gamma_\mathrm{C}B_z-A_z^j/2)^2+(A_x^j/2)^2+(A_y^j/2)^2}$.

We adjust the magnetic field to 100 G to demonstrate the efficiency of decoupling the quantum noise, as shown in Fig. 3(d). The signal of the ordinary Ramsey method is displayed in the top, labeled as S1. T_2^* is estimated to be 1.8(1) μs, and the beat pattern is caused by the strongly coupled ^{13}C nuclear spin and the unpolarized ^{14}N nuclear spin. After only decoupling the thermal noise, T_2^* is extended to 4.2(5) μs as shown in the middle (S2). The signal in the bottom (S3) is obtained by inserting eight R_z^π gates (four before the R^π and four after), and T_2^* is further extended to 7.8(9) μs. We simply use the function $S(\tau)=A\cos(\omega\tau+\phi)\mathrm{e}^{-(\tau/T_2^*)^2}+C$

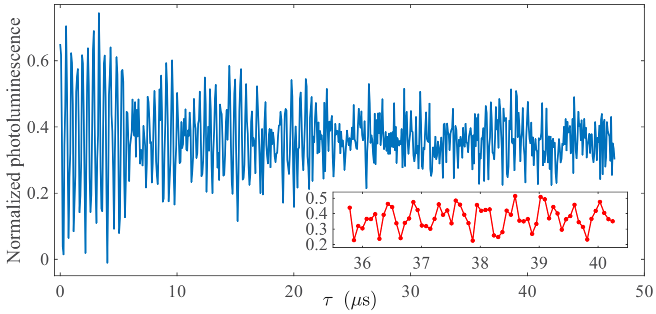

FIG. 4. Decoupling the thermal noise utilizing a stronger RF power. Inset: closeup for the signals around 40 μs.

to fit signals S2 and S3. We also perform numerical simulations at a weaker magnetic field by randomly generating configurations of ^{13}C bath including about 500 ^{13}C nuclear spins with 1.1% natural abundance, as shown in Appendix B.

V. CONCLUSION

We propose a method to extend T_2^* of a single NV center in a high-purity diamond sample with ^{13}C nuclear spins as the main dephasing source. Utilizing the intrinsic ^{14}N nuclear spin as the coherence register, we invert the ^{13}C nuclear spin bath to decouple its thermal noise at 455 G. The dephasing time T_2^* is extended from 2.6 to 5.4 μs by a hard pulse and 10.2 μs by a robust adiabatic pulse. Furthermore, we decouple the quantum noise to the first order by dividing the free evolution into pieces and inserting an R_z^π of the nuclear spin bath into every piece. Combining with the thermal noise decoupling, T_2^* is extended by more than four times at 100 G. Our findings provide a new avenue for investigating the dephasing mechanism caused by the nuclear spin bath [56,57]. These results have potential implications for exploring novel strategies for mitigating thermal and quantum noise in quantum information processing. Additionally, our proposal can also be readily adapted to a wide variety of other solid-state defects, such as silicon-vacancy center in diamond [58] and silicon carbide [59].

In terms of sensitivity, our method is primarily constrained by the extended duration of the inversion pulse, which reduces the benefits of dephasing time enhancement. Furthermore, the prolonged duration leads to an increase in magnetic drifts, thereby diminishing the efficiency of extension. Another factor that limits the performance of our method is the RF power. We increase the RF power to invert the spin bath and see oscillation around 40 μs, as shown in Appendix A. Therefore, a more effective design of the RF transmitter, such as implementing a coil circuit [60], will be beneficial to our method. As the dephasing time is further extended, the weak intrabath evolution, dominated by the flip-flop interactions between spin pairs [22], starts to influence the decoupling efficiency. To counteract this, we can repeat the decoupling process in the dashed box in Fig. 1(b).

ACKNOWLEDGMENTS

This work is supported by the National Natural Science Foundation of China under Grants No. 12204051, No. 11974205, and No. 11774197, and the Beijing Natural Science Foundation under Grant No. Z200009.

APPENDIX A: DETAILS OF DECOUPLING THE THERMAL NOISE

In the rotating frame of $U_{\rm rot} = {\rm e}^{i\omega_{\rm e} t S_z^2}$ and constructing the computational qubit $|0\rangle$ and $|1\rangle$ with $m_S = 0, -1$, Eq. (1) can be written as

$$H^{\rm eff}_{\rm e\text{-}C} = |0\rangle\langle 0|\sum_j \gamma_{\rm C} B_z I_z^j + |1\rangle\langle 1|\left(\sum_j \gamma_{\rm C} B_z I_z^j - \sum_j\sum_i A_i^j I_i^j + \Delta\right) = |0\rangle\langle 0|\sum_j H_0^j + |1\rangle\langle 1|\left(\sum_j H_1^j + \Delta\right), \tag{A1}$$

where $H_0^j = \gamma_{\rm C} B_z I_z^j$ and $H_1^j = \gamma_{\rm C} B_z I_z^j - \sum_i A_i^j I_i^j$ are the Hamiltonians of the jth ^{13}C nuclear spin when $m_S = 0$ and $m_S = -1$, and $\Delta = D - \omega_{\rm e} - \gamma_{\rm e} B_z$ is the detuning frequency. After the Ramsey measurement as described in Sec. II, the readout signal can be calculated as

$$S(\tau) = \frac{1}{2} - \frac{\cos\Delta\tau}{2}\prod_j {\rm Tr}\left[\frac{U_0^{j\dagger}(\tau) U_1^j(\tau)}{2}\right], \tag{A2}$$

where $U_0^j(\tau) = {\rm e}^{-iH_0^j\tau}$ and $U_1^j(\tau) = {\rm e}^{-iH_1^j\tau}$ are the evolution operators of the jth ^{13}C nuclear spin when $m_S = 0$ and $m_S = -1$, and τ is the free evolution time. The cumulative product in Eq. (A2) contributes an exponential decay [22]. We insert an inversion pulse in the middle of free evolution to decouple the thermal noise. Without loss of generality, we set the inversion pulse as R_x^π, and the cumulative product can be recast as

$$\begin{aligned}
&\prod_j \frac{1}{2}{\rm Tr}\big[U_0^{j\dagger}(\tau/2) R_{-x}^\pi U_0^{j\dagger}(\tau/2) U_1^j(\tau/2) R_x^\pi U_1^j(\tau/2)\big] \\
&= \prod_j \frac{1}{2}{\rm Tr}\big[R_{-x}^\pi {\rm e}^{-i(\gamma_{\rm C} B_z I_z^j - \sum_i A_i^j I_i^j)\tau/2} R_x^\pi {\rm e}^{-i(\gamma_{\rm C} B_z I_z^j - \sum_i A_i^j I_i^j)\tau/2}\big] = \prod_j \frac{1}{2}{\rm Tr}\big[{\rm e}^{i(\gamma_{\rm C} B_z I_z^j + A_x^j I_x^j - A_y^j I_y^j - A_z^j I_z^j)\tau/2}{\rm e}^{-i(\gamma_{\rm C} B_z I_z^j - A_x^j I_x^j - A_y^j I_y^j - A_z^j I_z^j)\tau/2}\big] \\
&\approx \prod_j \frac{1}{2}{\rm Tr}\big[{\rm e}^{i(\gamma_{\rm C} B_z - A_z^j)\tau I_z^j/2}{\rm e}^{-i(\gamma_{\rm C} B_z - A_z^j)\tau I_z^j/2}\big] = 1,
\end{aligned} \tag{A3}$$

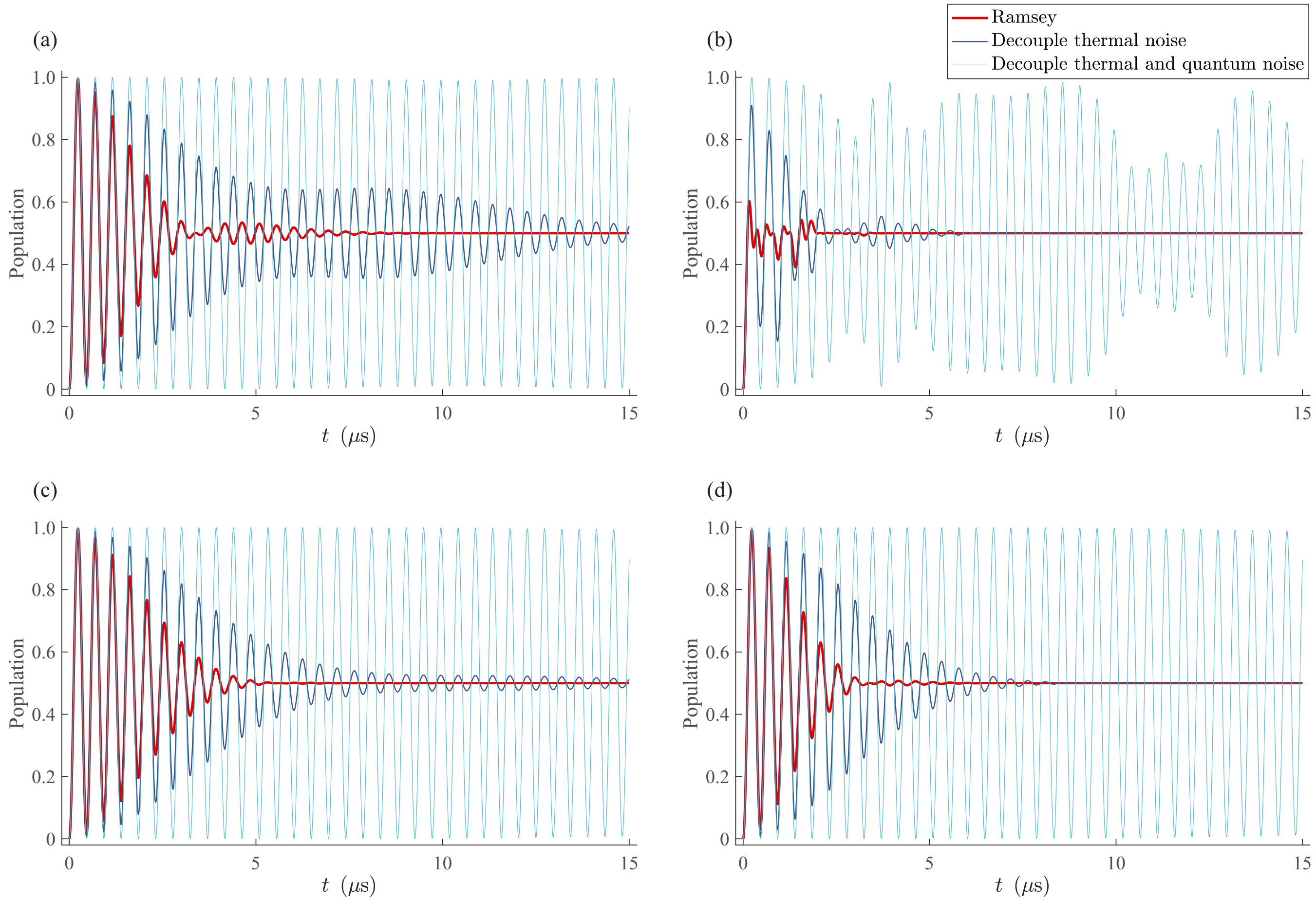

FIG. 5. Results of numerical simulations for four different spin baths (a)–(d). With a weak magnetic field of 50 G, the signal with the thermal noise decoupled is limited by the quantum noise. In contrast, by inserting eight R_z^π gates (four before the R^π and four after), the dephasing time is extended substantially.

where we neglect the off-diagonal part because a strong external magnetic field is considered here. For the same reason, when we use the decoupling procedure in Fig. 1(b), the evolution during the transfer operation can also be neglected. Equation (A3) shows that the thermal noise can be decoupled, and the experimental results are displayed in Fig. 2(d). We increase the RF power to invert the bath spins as shown in Fig. 4. The amplitude of the signal is increased compared to the main text, and an oscillation around 40 μs can be observed. However, we cannot have a proper fitting to the signal, and we mainly attribute it to the temperature drifts and magnetic fluctuations over the long experiment periods. Moreover, the signal comprises rich information about the ^{13}C bath, which requires further study.

APPENDIX B: DETAILS OF DECOUPLING THE QUANTUM NOISE

At a medium magnetic field, as shown in the Fig. 3, we can decouple the quantum noise by dividing the free evolution into N pieces and inserting an R_z^π gate on the ^{13}C nuclear spins in the middle of every piece. The divided free evolution is $[U^{\mathrm{d}}_{\text{e-C}}(\tau/2N)]^N$, and $U^{\mathrm{d}}_{\text{e-C}}(\tau/2N)$ can be described as

$$\begin{aligned}U^{\mathrm{d}}_{\text{e-C}}(\tau/2N) &= U_{\text{e-C}}(\tau/2N)\cdot \otimes_j R^\pi_{z,j}\cdot U_{\text{e-C}}(\tau/2N)\\ &= \left[|0\rangle\langle 0|\otimes_j U_0^j(\tau/4N)+|1\rangle\langle 1|\otimes_j U_1^j(\tau/4N)\right]\cdot\otimes_j R^\pi_{z,j}\cdot\left[|0\rangle\langle 0|\otimes_j U_0^j(\tau/4N)+|1\rangle\langle 1|\otimes_j U_1^j(\tau/4N)\right]\\ &= |0\rangle\langle 0|\otimes_j U_0^j(\tau/4N)\cdot R^\pi_{z,j}\cdot U_0^j(\tau/4N)+|1\rangle\langle 1|\otimes_j U_1^j(\tau/4N)\cdot R^\pi_{z,j}\cdot U_1^j(\tau/4N),\end{aligned} \tag{B1}$$

where we omit the detuning frequency, and we have

$$U_0^j(\tau/4N)\cdot R^\pi_{z,j}\cdot U_0^j(\tau/4N) = U_0^j(\tau/2N)\cdot R^\pi_{z,j} \tag{B2}$$

and

$$
\begin{aligned}
U_1^j(\tau/4N)\cdot R_{z,j}^{\pi}\cdot U_1^j(\tau/4N) &= \mathrm{e}^{-i(\gamma_C B_z I_z^j - A_x^j I_x^j - A_y^j I_y^j - A_z^j I_z^j)\tau/4N}\cdot R_{z,j}^{\pi}\cdot \mathrm{e}^{-i(\gamma_C B_z I_z^j - A_x^j I_x^j - A_y^j I_y^j - A_z^j I_z^j)\tau/4N}\\
&= \mathrm{e}^{-i(\gamma_C B_z I_z^j - A_x^j I_x^j - A_y^j I_y^j - A_z^j I_z^j)\tau/4N}\mathrm{e}^{-i(\gamma_C B_z I_z^j + A_x^j I_x^j + A_y^j I_y^j - A_z^j I_z^j)\tau/4N}\cdot R_{z,j}^{\pi}\\
&\approx \big[\mathbb{I} - i\big(\gamma_C B_z I_z^j - A_x^j I_x^j - A_y^j I_y^j - A_z^j I_z^j\big)\tau/4N\big]\big[\mathbb{I} - i\big(\gamma_C B_z I_z^j + A_x^j I_x^j + A_y^j I_y^j - A_z^j I_z^j\big)\tau/4N\big]\cdot R_{z,j}^{\pi}\\
&\approx \big[\mathbb{I} - i\big(\gamma_C B_z I_z^j - A_z^j I_z^j\big)\tau/2N\big]\cdot R_{z,j}^{\pi}. \qquad \text{(B3)}
\end{aligned}
$$

We can see that the off-diagonal part is decoupled to the first order. The approximations hold true when $A_{x/y/z}^j\tau/4N \ll 1$. So we can get a better decoupling effect by dividing the whole evolution into more pieces.

With regard to the numerical simulations, we randomly generate four configurations of ^{13}C bath, including about 500 ^{13}C nuclear spins with 1.1% natural abundance. For simplicity, we only consider the dipole-dipole interactions with the electron spin. The R_z^{π} gate can be achieved by a free precession of duration $\pi/\gamma_C B_z$, as described in the main text. By utilizing a conditional gate, we can drive the electron spin to $|0\rangle_e$, causing all the ^{13}C nuclear spins to precess at a speed of $\gamma_C B_z$. Here we assume that the R_z^{π} gates are ideal, so that the dynamics of the system is solvable. The simulation results are shown in Fig. 5. With a weak magnetic field of 50 G, the signal with the thermal noise decoupled is limited by the quantum noise. However, by inserting eight R_z^{π} gates (four before the R^{π} and four after), the dephasing time is extended substantially.

[1] C. L. Degen, F. Reinhard, and P. Cappellaro, Quantum sensing, Rev. Mod. Phys. **89**, 035002 (2017).

[2] J. F. Barry, J. M. Schloss, E. Bauch, M. J. Turner, C. A. Hart, L. M. Pham, and R. L. Walsworth, Sensitivity optimization for NV-diamond magnetometry, Rev. Mod. Phys. **92**, 015004 (2020).

[3] P. Rembold, N. Oshnik, M. M. Müller, S. Montangero, T. Calarco, and E. Neu, Introduction to quantum optimal control for quantum sensing with nitrogen-vacancy centers in diamond, AVS Quantum Sci. **2**, 024701 (2020).

[4] G. Balasubramanian, I. Y. Chan, R. Kolesov, M. Al-Hmoud, J. Tisler, C. Shin, C. Kim, A. Wojcik, P. R. Hemmer, A. Krueger, T. Hanke, A. Leitenstorfer, R. Bratschitsch, F. Jelezko, and J. Wrachtrup, Nanoscale imaging magnetometry with diamond spins under ambient conditions, Nature (London) **455**, 648 (2008).

[5] J. R. Maze, P. L. Stanwix, J. S. Hodges, S. Hong, J. M. Taylor, P. Cappellaro, L. Jiang, M. V. G. Dutt, E. Togan, A. S. Zibrov, A. Yacoby, R. L. Walsworth, and M. D. Lukin, Nanoscale magnetic sensing with an individual electronic spin in diamond, Nature (London) **455**, 644 (2008).

[6] Y.-X. Liu, A. Ajoy, and P. Cappellaro, Nanoscale vector dc magnetometry via ancilla-assisted frequency up-conversion, Phys. Rev. Lett. **122**, 100501 (2019).

[7] F. Dolde, H. Fedder, M. W. Doherty, T. Nöbauer, F. Rempp, G. Balasubramanian, T. Wolf, F. Reinhard, L. C. L. Hollenberg, F. Jelezko, and J. Wrachtrup, Electric-field sensing using single diamond spins, Nat. Phys. **7**, 459 (2011).

[8] M. S. J. Barson, P. Peddibhotla, P. Ovartchaiyapong, K. Ganesan, R. L. Taylor, M. Gebert, Z. Mielens, B. Koslowski, D. A. Simpson, L. P. McGuinness, J. McCallum, S. Prawer, S. Onoda, T. Ohshima, A. C. Bleszynski Jayich, F. Jelezko, N. B. Manson, and M. W. Doherty, Nanomechanical sensing using spins in diamond, Nano Lett. **17**, 1496 (2017).

[9] V. M. Acosta, E. Bauch, M. P. Ledbetter, A. Waxman, L.-S. Bouchard, and D. Budker, Temperature dependence of the nitrogen-vacancy magnetic resonance in diamond, Phys. Rev. Lett. **104**, 070801 (2010).

[10] G. Kucsko, P. C. Maurer, N. Y. Yao, M. Kubo, H. J. Noh, P. K. Lo, H. Park, and M. D. Lukin, Nanometre-scale thermometry in a living cell, Nature (London) **500**, 54 (2013).

[11] G.-Q. Liu, X. Feng, N. Wang, Q. Li, and R.-B. Liu, Coherent quantum control of nitrogen-vacancy center spins near 1000 kelvin, Nat. Commun. **10**, 1344 (2019).

[12] M. W. Doherty, V. V. Struzhkin, D. A. Simpson, L. P. McGuinness, Y. Meng, A. Stacey, T. J. Karle, R. J. Hemley, N. B. Manson, L. C. L. Hollenberg, and S. Prawer, Electronic properties and metrology applications of the diamond NV center under pressure, Phys. Rev. Lett. **112**, 047601 (2014).

[13] B. Dellabetta, T. L. Hughes, M. J. Gilbert, and B. L. Lev, Imaging topologically protected transport with quantum degenerate gases, Phys. Rev. B **85**, 205442 (2012).

[14] E. M. Spanton, K. C. Nowack, L. Du, G. Sullivan, R.-R. Du, and K. A. Moler, Images of edge current in InAs/GaSb quantum wells, Phys. Rev. Lett. **113**, 026804 (2014).

[15] I. Gross, W. Akhtar, V. Garcia, L. Martínez, S. Chouaieb, K. Garcia, C. Carrétéro, A. Barthélémy, P. Appel, P. Maletinsky, J. Kim, J. Chauleau, N. Jaouen, M. Viret, M. Bibes, S. Fusil, and V. Jacques, Real-space imaging of non-collinear antiferromagnetic order with a single-spin magnetometer, Nature (London) **549**, 252 (2017).

[16] J. P. Wikswo, J. P. Barach, and J. A. Freeman, Magnetic field of a nerve impulse: First measurements, Science **208**, 53 (1980).

[17] J. F. Barry, M. J. Turner, J. M. Schloss, D. R. Glenn, Y. Song, M. D. Lukin, H. Park, and R. L. Walsworth, Optical magnetic detection of single-neuron action potentials using quantum defects in diamond, Proc. Natl. Acad. Sci. USA **113**, 14133 (2016).

[18] K. Jensen, R. Budvytyte, R. A. Thomas, T. Wang, A. M. Fuchs, M. V. Balabas, G. Vasilakis, L. D. Mosgaard, H. C. Stærkind, J. H. Müller, T. Heimburg, S.-P. Olesen, and E. S. Polzik, Non-invasive detection of animal nerve impulses with an atomic magnetometer operating near quantum limited sensitivity, Sci. Rep. **6**, 29638 (2016).

[19] N. F. Ramsey, A molecular beam resonance method with separated oscillating fields, Phys. Rev. **78**, 695 (1950).

[20] E. Togan, Y. Chu, A. Imamoglu, and M. D. Lukin, Laser cooling and real-time measurement of the nuclear spin environment of a solid-state qubit, Nature (London) **478**, 497 (2011).

[21] A. Dréau, P. Jamonneau, O. Gazzano, S. Kosen, J.-F. Roch, J. R. Maze, and V. Jacques, Probing the dynamics of a nuclear spin bath in diamond through time-resolved central spin magnetometry, Phys. Rev. Lett. **113**, 137601 (2014).

[22] N. Zhao, S.-W. Ho, and R.-B. Liu, Decoherence and dynamical decoupling control of nitrogen vacancy center electron spins in nuclear spin baths, Phys. Rev. B **85**, 115303 (2012).

[23] R. Hanson, V. Dobrovitski, A. Feiguin, O. Gywat, and D. Awschalom, Coherent dynamics of a single spin interacting with an adjustable spin bath, Science **320**, 352 (2008).

[24] G.-Q. Liu, X.-Y. Pan, Z.-F. Jiang, N. Zhao, and R.-B. Liu, Controllable effects of quantum fluctuations on spin free-induction decay at room temperature, Sci. Rep. **2**, 432 (2012).

[25] P. London, J. Scheuer, J.-M. Cai, I. Schwarz, A. Retzker, M. B. Plenio, M. Katagiri, T. Teraji, S. Koizumi, J. Isoya, R. Fischer, L. P. McGuinness, B. Naydenov, and F. Jelezko, Detecting and polarizing nuclear spins with double resonance on a single electron spin, Phys. Rev. Lett. **111**, 067601 (2013).

[26] G.-Q. Liu, Q.-Q. Jiang, Y.-C. Chang, D.-Q. Liu, W.-X. Li, C.-Z. Gu, H. C. Po, W.-X. Zhang, N. Zhao, and X.-Y. Pan, Protection of centre spin coherence by dynamic nuclear spin polarization in diamond, Nanoscale **6**, 10134 (2014).

[27] I. Schwartz, J. Scheuer, B. Tratzmiller, S. Müller, Q. Chen, I. Dhand, Z.-Y. Wang, C. Müller, B. Naydenov, F. Jelezko, and B. Plenio, Robust optical polarization of nuclear spin baths using hamiltonian engineering of nitrogen-vacancy center quantum dynamics, Sci. Adv. **4**, eaat8978 (2018).

[28] J. Scheuer, I. Schwartz, S. Müller, Q. Chen, I. Dhand, M. B. Plenio, B. Naydenov, and F. Jelezko, Robust techniques for polarization and detection of nuclear spin ensembles, Phys. Rev. B **96**, 174436 (2017).

[29] Q. Chen, I. Schwarz, F. Jelezko, A. Retzker, and M. B. Plenio, Optical hyperpolarization of ^{13}C nuclear spins in nanodiamond ensembles, Phys. Rev. B **92**, 184420 (2015).

[30] J. Scheuer, I. Schwartz, Q. Chen, D. Schulze-Sünninghausen, P. Carl, P. Höfer, A. Retzker, H. Sumiya, J. Isoya, B. Luy, M. B. Plenio, B. Naydenov, and F. Jelezko, Optically induced dynamic nuclear spin polarisation in diamond, New J. Phys. **18**, 013040 (2016).

[31] G. Balasubramanian, P. Neumann, D. Twitchen, M. Markham, R. Kolesov, N. Mizuochi, J. Isoya, J. Achard, J. Beck, J. Tissler, V. Jacques, P. R. Hemmer, F. Jelezko, and J. Wrachtrup, Ultralong spin coherence time in isotopically engineered diamond, Nat. Mater. **8**, 383 (2009).

[32] E. D. Herbschleb, H. Kato, Y. Maruyama, T. Danjo, T. Makino, S. Yamasaki, I. Ohki, K. Hayashi, H. Morishita, M. Fujiwara, and N. Mizuochi, Ultra-long coherence times amongst room-temperature solid-state spins, Nat. Commun. **10**, 3766 (2019).

[33] G. de Lange, T. Van Der Sar, M. Blok, Z.-H. Wang, V. Dobrovitski, and R. Hanson, Controlling the quantum dynamics of a mesoscopic spin bath in diamond, Sci. Rep. **2**, 382 (2012).

[34] H. S. Knowles, D. M. Kara, and M. Atatüre, Observing bulk diamond spin coherence in high-purity nanodiamonds, Nat. Mater. **13**, 21 (2014).

[35] E. Bauch, C. A. Hart, J. M. Schloss, M. J. Turner, J. F. Barry, P. Kehayias, S. Singh, and R. L. Walsworth, Ultralong dephasing times in solid-state spin ensembles via quantum control, Phys. Rev. X **8**, 031025 (2018).

[36] S. Zaiser, T. Rendler, I. Jakobi, T. Wolf, S.-Y. Lee, S. Wagner, V. Bergholm, T. Schulte-Herbrüggen, P. Neumann, and J. Wrachtrup, Enhancing quantum sensing sensitivity by a quantum memory, Nat. Commun. **7**, 12279 (2016).

[37] M. Pfender, N. Aslam, H. Sumiya, S. Onoda, P. Neumann, J. Isoya, C. A. Meriles, and J. Wrachtrup, Nonvolatile nuclear spin memory enables sensor-unlimited nanoscale spectroscopy of small spin clusters, Nat. Commun. **8**, 834 (2017).

[38] V. Jacques, P. Neumann, J. Beck, M. Markham, D. Twitchen, J. Meijer, F. Kaiser, G. Balasubramanian, F. Jelezko, and J. Wrachtrup, Dynamic polarization of single nuclear spins by optical pumping of nitrogen-vacancy color centers in diamond at room temperature, Phys. Rev. Lett. **102**, 057403 (2009).

[39] B. Smeltzer, J. McIntyre, and L. Childress, Robust control of individual nuclear spins in diamond, Phys. Rev. A **80**, 050302(R) (2009).

[40] M. Steiner, P. Neumann, J. Beck, F. Jelezko, and J. Wrachtrup, Universal enhancement of the optical readout fidelity of single electron spins at nitrogen-vacancy centers in diamond, Phys. Rev. B **81**, 035205 (2010).

[41] G.-Q. Liu, H. C. Po, J. Du, R.-B. Liu, and X.-Y. Pan, Noise-resilient quantum evolution steered by dynamical decoupling, Nat. Commun. **4**, 2254 (2013).

[42] G. Waldherr, Y. Wang, S. Zaiser, M. Jamali, T. Schulte-Herbrüggen, H. Abe, T. Ohshima, J. Isoya, J. F. Du, P. Neumann, and J. Wrachtrup, Quantum error correction in a solid-state hybrid spin register, Nature (London) **506**, 204 (2014).

[43] T. van der Sar, Z. H. Wang, M. S. Blok, H. Bernien, T. H. Taminiau, D. M. Toyli, D. A. Lidar, D. D. Awschalom, R. Hanson, and V. V. Dobrovitski, Decoherence-protected quantum gates for a hybrid solid-state spin register, Nature (London) **484**, 82 (2012).

[44] C. E. Bradley, J. Randall, M. H. Abobeih, R. C. Berrevoets, M. J. Degen, M. A. Bakker, M. Markham, D. J. Twitchen, and T. H. Taminiau, A ten-qubit solid-state spin register with quantum memory up to one minute, Phys. Rev. X **9**, 031045 (2019).

[45] See Supplemental Material at http://link.aps.org/supplemental/10.1103/PhysRevB.108.174111 for details on the experimental techniques employed to obtain the results presented in the main text.

[46] T. H. Taminiau, J. Cramer, T. van der Sar, V. V. Dobrovitski, and R. Hanson, Universal control and error correction in multi-qubit spin registers in diamond, Nat. Nanotechnol. **9**, 171 (2014).

[47] T. H. Taminiau, J. J. T. Wagenaar, T. van der Sar, F. Jelezko, V. V. Dobrovitski, and R. Hanson, Detection and control of individual nuclear spins using a weakly coupled electron spin, Phys. Rev. Lett. **109**, 137602 (2012).

[48] S. Kolkowitz, Q. P. Unterreithmeier, S. D. Bennett, and M. D. Lukin, Sensing distant nuclear spins with a single electron spin, Phys. Rev. Lett. **109**, 137601 (2012).

[49] N. Zhao, J. Honert, B. Schmid, M. Klas, J. Isoya, M. Markham, D. Twitchen, F. Jelezko, R.-B. Liu, H. Fedder, and J. Wrachtrup, Sensing single remote nuclear spins, Nat. Nanotechnol. **7**, 657 (2012).

[50] L. Childress, M. V. Gurudev Dutt, J. M. Taylor, A. S. Zibrov, F. Jelezko, J. Wrachtrup, P. R. Hemmer, and M. D. Lukin, Coherent dynamics of coupled electron and nuclear spin qubits in diamond, Science **314**, 281 (2006).

[51] E. Kupce and R. Freeman, Adiabatic pulses for wideband inversion and broadband decoupling, J. Magn. Reson., Ser. A **115**, 273 (1995).

[52] L. A. O'Dell, The WURST kind of pulses in solid-state NMR, Solid State Nucl. Magn. Reson. **55-56**, 28 (2013).

[53] S. Tabatabaei, H. Haas, W. Rose, B. Yager, M. Piscitelli, P. Sahafi, A. Jordan, P. J. Poole, D. Dalacu, and R. Budakian, Numerical engineering of robust adiabatic operations, Phys. Rev. Appl. **15**, 044043 (2021).

[54] T. Gullion, D. B. Baker, and M. S. Conradi, New, Compensated Carr-Purcell sequences, J. Magn. Reson. **89**, 479 (1990).

[55] A. M. Souza, G. A. Álvarez, and D. Suter, Robust dynamical decoupling, Philos. Trans. R. Soc. A. **370**, 4748 (2012).

[56] P. Huang, X. Kong, N. Zhao, F. Shi, P. Wang, X. Rong, R.-B. Liu, and J. Du, Observation of an anomalous decoherence effect in a quantum bath at room temperature, Nat. Commun. **2**, 570 (2011).

[57] F. Reinhard, F. Shi, N. Zhao, F. Rempp, B. Naydenov, J. Meijer, L. T. Hall, L. Hollenberg, J. Du, R.-B. Liu, and J. Wrachtrup, Tuning a spin bath through the quantum-classical transition, Phys. Rev. Lett. **108**, 200402 (2012).

[58] B. Pingault, D.-D. Jarausch, C. Hepp, L. Klintberg, J. N. Becker, M. Markham, C. Becher, and M. Atatüre, Coherent control of the silicon-vacancy spin in diamond, Nat. Commun. **8**, 15579 (2017).

[59] R. Nagy, M. Niethammer, M. Widmann, Y.-C. Chen, P. Udvarhelyi, C. Bonato, J. U. Hassan, R. Karhu, I. G. Ivanov, N. T. Son, J. R. Maze, T. Ohshima, Ö. O. Soykal, Á. Gali, S.-Y. Lee, F. Kaiser, and J. Wrachtrup, High-fidelity spin and optical control of single silicon-vacancy centres in silicon carbide, Nat. Commun. **10**, 1954 (2019).

[60] K. Herb, J. Zopes, K. S. Cujia, and C. L. Degen, Broadband radio-frequency transmitter for fast nuclear spin control, Rev. Sci. Instrum. **91**, 113106 (2020).